PERGAMON

Vacuum 67 (2002) 673–686

VACUUM
SURFACE ENGINEERING, SURFACE INSTRUMENTATION & VACUUM TECHNOLOGY

www.elsevier.com/locate/vacuum

Energetic deposition using filtered cathodic arc plasmas

André Anders*

Lawrence Berkeley National Laboratory, University of California, 1 Cyclotron Road, Mailstop 53, Berkeley, CA 94720, USA

Abstract

Energetic film deposition techniques, film properties, and some applications are briefly reviewed. Energetic deposition can be defined as a film deposition process in which a significant fraction of particles arrives at the substrate surface with a kinetic energy greater than the bulk displacement energy. Examples of energetic deposition processes include ion-beam-assisted deposition, plasma immersion ion deposition, pulsed laser deposition, and cathodic arc deposition. This work focuses on the production, properties, and use of filtered cathodic arc plasmas. The pulsed biasing technique of metal plasma immersion ion implantation and deposition extends the possibilities of tuning film properties such as density, stress, adhesion, surface roughness, hardness, elastic modulus, and optical constants via the energy of film-forming ions. The difference between kinetic and total ion energy, atomic scale heating, nucleation, intermixing, subplantation, and the relaxation of compressive stress by relatively high-energy ions are discussed.

Keywords: Energetic deposition; Metal plasma immersion ion implantation and deposition (MePIIID); Film stress; Adhesion; Filtered cathodic arc; Subplantation; Atomic scale heating; Review

1. Introduction

The surface properties are generally critical for the use of components in many applications. Surface engineering has become a field of intense research. Among the many technologies, plasma-assisted or plasma-based techniques of surface modification and thin film deposition are widely used. The relatively simple thermal and electron-beam evaporation techniques are characterized by high rates and low-particle energies (<1 eV). They are often used for large-area, thick (μm) coatings that have a porous microstructure with tensile stress. Sputtering techniques produce particles of higher energy (5–10 eV), leading to denser films with less tensile stress at a high pressure, or even compressive stress at low-sputtering pressure.

In sputtering, partially ionized plasma is present, allowing the operator to apply substrate biasing thereby manipulating the energy of particles that form the film or assist film growth. In conjunction with a suitable substrate temperature, film properties can be adjusted in a wide range. A variety of sputtering techniques (magnetron, unbalanced magnetron, ionized sputtering, pulsed sputtering, ion beam sputtering, etc.) have been developed, now dominating the field of thin film coating [1,2].

Energetic deposition can be defined as a film deposition process in which a significant fraction of particles arrives at the substrate surface with a kinetic energy greater than the bulk displacement energy of the substrate. The bulk displacement

*Tel.: +1-510-4866745; fax: +1-510-4864374.
E-mail address: aanders@lbl.gov (A. Anders).

0042-207X/02/$ - see front matter
PII: S0042-207X(02)00260-9

energy is generally defined as the energy needed to move a substrate atom from its bulk lattice site to a stable interstitial site. The bulk displacement energy is not well defined because it depends on the direction of the energetic particle causing the displacement relative to the crystalline texture, if the material is crystalline. For amorphous materials, the terms "interstitial" and "vacancy" are not exactly applicable and can only be understood in the sense of local density. Therefore, a range of energies exists for the creation of a Frenkel pair (interstitial and vacancy). Displacement energies are in the range from about 10 eV for magnesium to about 40 eV for rhenium [3]. The uncertainty in the definition of the displacement energy is not of great concern here because it only determines the lower energy limit of "energetic deposition."

The energetic particle fraction can be supplied by a dedicated source of energetic particles, usually ions, or the film-forming particles themselves may be energetic. For example, the supersonic flux of cathodic arc-generated ions can be considered as a self-ion-assisted process.

To obtain an overview of this field, the paper is organized as follows. In Section 2, energetic film growth techniques are systematically discussed with emphasis on filtered cathodic arc plasmas and the technique of metal plasma immersion ion implantation and deposition (MePIIID). This is followed by considerations of energetic film growth and film properties, and finally some applications are briefly discussed.

2. Techniques of energetic film deposition

2.1. Ion-beam deposition

Ion beams can be formed in ion sources using a plasma-generating system (such as a filament, radio frequency (RF), or microwave discharge) and an ion extraction system. One may distinguish between broad-beam deposition and mass-selected ion-beam deposition.

In the broad beam concept, a space–charge-compensated ion beam of film-forming species is directed to the substrate. The most prominent example is the ion beam deposition of diamond-like carbon (DLC or a-C:H), where a hydrocarbon-containing gas mixture is used in the ion source. The ion energy here is typically 100 eV, i.e. low energy from an ion-beam point of view, but energetic from a deposition point of view.

In mass-selected ion beam deposition, a beam of positive and/or negative ions of much higher energy (many keV) is sent through a magnetic system allowing the operator to pick the desired ion species from the species present in the original beam. The flux of selected species is decelerated to the desired energy before impacting the substrate. Mass-selected ion beam deposition is a great tool for fundamental research (e.g. [4–7]), but not suitable for coating production due to very high cost and small coating area.

2.2. Ion-beam-assisted deposition (IBAD)

It is well known that with evaporation and sputter deposition, ion beam assistance can greatly alter the film properties. In essence, the growing film is bombarded with energetic ions, often argon, generated by a dedicated ion source such as a Kaufman, or gridless, or End–Hall ion source. The film properties are greatly influenced by the ion energy and the ion-to-atom arrival ratio. Many reviews and books deal with IBAD (e.g. [1,8,9]) and thus here we will not repeat the findings but borrow from the knowledge when later discussing the effects of self-ion assistance by the techniques described in the following sections.

2.3. Ionized and pulsed magnetron sputtering

Depending on the sputtering pressure, sputter deposition may or may not be considered as energetic deposition in the above-defined sense. Most sputtered particles have energy of a few eV; thus, sputter deposition is not energetic deposition, at least at high sputter pressure. However, at a low pressure, the energetic tail of the distribution (10–100 eV) may become decisive for the film properties. The degree of ionization of the sputter plasma is low ($<1\%$) and therefore substrate biasing, if applied, influences only a small fraction of particles. This drawback is mitigated by special means of enhancing the degree of ionization such

as additional RF plasma heating [10,11] or pulsed-DC plasma heating [12]. With enhanced degree of ionization, substrate biasing can lead to "plasma-assisted" or more exactly "ion-assisted" film growth in the sense of energetic deposition. Energetic sputtering methods are being used to deposit hard and superhard films and nanocomposite coatings [13]. The mechanism of energetic ion generation by substrate bias is explained in more detail in the section on plasma immersion techniques (2.6).

2.4. Pulsed laser plasma deposition

Pulsed laser ablation of material for a solid target involves the generation of plasma of the ablated material [14], and this plasma is often characterized by a high degree of ionization and kinetic ion energy [15,16]. Since the laser pulse length is usually short (μs or even less), the duty cycle is low even at high-pulse repetition rates, and average deposition rates are low. Pulsed laser deposition is the method of choice for some specialty applications such as the deposition of high-temperature superconductors where criteria other than rate are important.

2.5. Cathodic (vacuum) arc plasma deposition

While laser ablation essentially works with all solid target materials, cathodic arc plasma deposition is limited to conducting materials. The consumable cathode is transferred to the plasma state at microscopic, non-stationary cathode spots—locations of extremely high-current density, power density, and plasma density [17]. The plasma expanding from cathode spots contains ions that are usually multiply charged and have a kinetic energy in the range 18–150 eV, depending on the cathode material (Table 1). The higher the cohesive energy of the solid cathode, the greater are the arc burning voltage, power density, average ion charge state, electron temperature, and ion kinetic energy (cohesive energy rule [18]). Cathodic arc plasma deposition is perhaps the oldest technique of energetic deposition [19].

Due to the explosive nature of plasma formation, cathodic arc processes also produce unwanted droplets and debris particles in the μm- and sub-μm range, commonly referred to as macroparticles. For some applications, such as reactive deposition of decorative and protective coatings such as TiN and (Ti,Al)N, macroparticles can be tolerated. For high-tech applications, macroparticles must be removed, while filtering is the most common approach. The original concept was introduced in the 1970s by Aksenov and coworkers [20], and about a dozen filter variations have been reviewed recently [21]. There are efforts to use filtered coating systems even for the traditional reactive arc deposition of TiN and (Ti,Al)N [22].

2.6. Metal plasma immersion ion implantation and deposition (MePIIID)

Even without substrate bias, cathodic arc plasma deposition is an energetic deposition, because the ion kinetic energy is high enough to cause the arriving ion to penetrate the substrate surface and to displace near-surface atoms. The range of ion energies can be greatly influenced by applying substrate bias. Here it is implied that the substrate is conducting. The situation is altered when the substrate or the growing film is insulating, see below.

Historically, biasing the substrate for energetic film growth was developed from two directions. In the first, a DC or RF bias voltage was applied to the substrate and the to-be-deposited vapor was partially ionized. This concept, introduced in the 1960s by Mattox as ion plating ([23] and references therein), was combined with various methods of vapor and plasma generation. It may be considered as the original approach to intentional energetic deposition. In a second route, pulsed high-voltage substrate biasing was introduced for implantation of metal ions [24] and gaseous ions [25]. The technique is today known as plasma immersion ion implantation and under several other names [26]. Brown and coworkers [27,28] extended the pulsed ion implantation concept to a hybrid ion implantation and deposition technique using vacuum arcs, presently known as metal plasma immersion ion implantation and deposition (MePIIID) [29]. In some sense, MePIIID can

Table 1
Cohesive energy [88], displacement energy [3], burning voltage at 300 A [18], kinetic energies [89], charge states (particle fractions) [90], and ionization energies [60,61] for selected cathodic arc plasmas

Cathode material	Cohesive energy (eV/atom)	Displ. energy (eV)	Arc burning voltage (V)	Kinetic ion energy (eV)	E_0 (eV)	$f(1+)(\%)$	E_1 (eV)	$f(2+)$ (%)	E_2 (eV)	$f(3+)$ (%)	E_3 (eV)	$f(4+)$ (%)	E_4 (eV)	$f(5+)$ (%)
Li	1.63		23.5	19	5.39	100	75.64	0		0		0		0
C (graphite)	7.37	25	29.6	19	11.3	100	24.38	0		0		0		0
Mg	1.51	10	18.8	49	7.65	46	15.04	54	80.14	0		0		0
Al	3.39	16	23.6	33	5.99	38	18.83	51	28.45	11	120.0	0		0
Si	4.63	13	27.5	34	8.15	63	16.35	35	33.49	2	45.14	0		0
Ti	4.85	19	21.3	59	6.83	11	13.76	75	27.49	14	43.27	0		0
V	5.31	26	22.5	70	6.75	8	14.66	71	29.31	20	46.71	1	65.28	0
Cr	4.1	28	22.9	71	6.77	10	16.49	68	30.96	21	49.16	1	69.46	0
Fe	4.28	17	22.7	46	7.90	25	16.19	68	30.65	7	54.80	0		0
Co	4.39	22	22.8	44	7.88	34	17.08	59	33.50	7	51.30	0		0
Ni	4.44	23	20.5	41	7.64	30	18.17	64	35.19	6	54.90	0		0
Cu	3.49	19	23.4	57	7.73	16	20.29	63	36.84	20	57.38	1	79.80	0
Zn	1.35	14	15.5	36	9.39	80	17.96	20	39.72	0		0		0
Ge	3.85	15	17.5	45	7.90	60	15.93	40	34.22	0		0		0
Y	4.37		18.1	80	6.22	5	12.24	62	20.52	33	60.60	0		0
Zr	6.25	21	23.4	112	6.63	1	13.13	47	22.99	45	34.34	7	80.35	0
Nb	7.57	28	27.0	128	6.76	1	14.32	24	25.04	51	38.30	22	50.55	2
Mo	6.82	33	29.3	149	7.09	2	16.16	21	27.13	49	46.40	25	54.49	3
Pd	3.89	26	21.3	131	8.34	23	19.43	67	32.93	9	60.87	1	78.25	0
Ag	2.95	23	23.0	69	7.58	13	21.49	61	34.83	25	60.52	1	80.01	0
Cd	1.16	19	16.0	27	8.99	68	16.91	32	37.48	0		0		0
In	2.52	15	17.5	21	5.79	66	18.87	34	28.03	0		0		0
Sn	3.14	22	17.5	30	7.34	47	14.63	53	30.50	0		0		0
Ta	8.1	32	28.7	136	7.89	2	14.47	33	23.49	38	36.32	24	49.14	3
W	8.9	38	31.9	117	7.98	2	15.08	23	25.43	43	39.29	26	53.15	6
Pt	5.84	33	22.5	67	9.00	12	19.24	69	35.25	18	51.27	1	67.28	0
Au	3.81	36	19.7	49	9.23	14	20.50	75	37.37	11	54.80	0		0
Pb	2.03		15.5	35	7.42	36	15.03	64	31.94	0		0		0
Bi	2.18		15.6	24	7.29	83	16.69	17	26.85	0		0		0
Th	6.2		23.3	118	6.08	0	11.50	24	20.00	64	28.80	12	57.22	0
U	5.55		23.5	160	6.19	20	11.63	40	18.09	32	30.90	8	49.91	0

The uranium charge state distribution was taken from [91]. The burning voltage, kinetic energies, and ion charge state distributions are values averaged over many discharges, thereby not showing the fluctuating nature of these values. The ionization energies are conventionally defined as E_0 for the energy to ionize the neutral, and E_1 to remove an electron from the singly charged ion forming a doubly charged ion, etc.

be understood as ion plating with cathodic arc plasmas and pulsed biasing. Pulsed biasing, as opposed to DC or RF, offers the advantage of additional process parameters such as pulse duration and duty cycle. Moreover, higher voltages can be applied, if desired, while the danger of unwanted substrate arcing is low.

Fig. 1 shows the general setup of MePIIID, using filtered vacuum arc plasma and pulsed biasing. The arc may be pulsed or continuous, and the bias is usually pulsed. During the pulse-off times, a film is formed by the condensing metal plasma. In the pulse-on time, plasma ions are accelerated in the space–charge sheath that forms between substrate and plasma. Ions are implanted more or less deeply; their projected range depends of course on the bias amplitude. Due to sputtering, surface material is removed and thus MePIIID does not always lead to film growth [30].

The kinetic energy of ions of charge state Q arriving at the substrate surface is time dependent and can be approximated by

$$E_{kin}(Q,t) = E_{kin,0} + QV_{bias}(t), \quad (1)$$

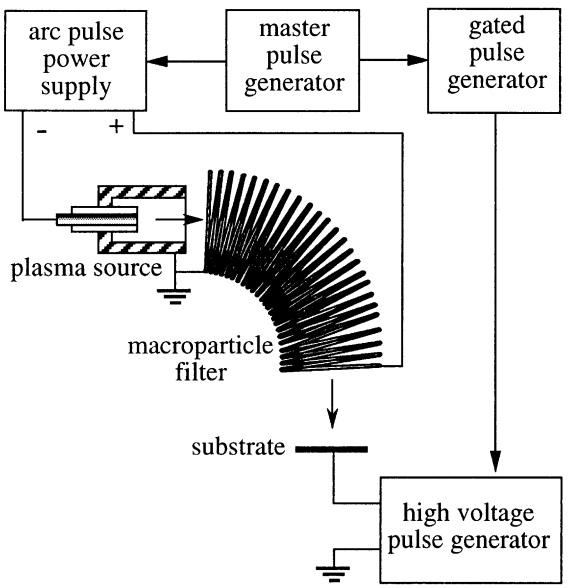

Fig. 1. Principal setup of metal plasma immersion ion implantation and deposition (MePIIID) using a filtered vacuum arc and pulse biasing.

where $E_{kin,0}$ is the kinetic energy the ion has acquired in the acceleration zone at the cathode spot, Q is the ion charge state number, and $V_{bias}(t)$ is the absolute value of time-dependent (negative) bias voltage. Experimentally, it has been found that $E_{kin,0}$ practically does not depend on the charge state [31]. Examples of kinetic energies and ion charge state distributions for selected cathodic arc plasmas are given in Table 1.

In the simplest case, the bias voltage has a rectangular shape with negligible rise and fall time. Suppose we consider the deposition of gold ions from a vacuum arc and use, for example, a pulsed bias voltage of -100 V. The kinetic energy distribution is then discrete with 14% at 134 eV, 75% at 234 eV and 11% at 334 eV (Fig. 2, top). Taking finite pulse rise and fall times into account, we obtain a more realistic distribution as shown in the center of Fig. 2. Additionally, one should keep in mind that charge state distributions fluctuate, thus, the distribution as shown in the figure would fluctuate as well. It is clear that MePIIID is not a monoenergetic process. This is generally acceptable for the deposition process, but it complicates the discussion and calculation of energy effects on film properties.

The use of filtered vacuum arc plasmas is advantageous for several reasons. Among them is the fact that the plasma is fully ionized, thus biasing influences all ions and not only a fraction of the incoming film-forming particles. The presence of multiply charged ions leads to greater ion kinetic energy, or the operator can choose to use a lower bias voltage, saving bias supply costs, reducing secondary electron emission, and reducing the risk of substrate arcing. Of particular interest in this respect are pulsed plasmas because their ion charge states are enhanced compared to steady-state conditions [32].

MePIIID with insulating substrates is not straightforward because bias cannot be directly applied. One can bias the holder thereby creating a sheath that facilitates ion acceleration, but ion energy is less, the geometry options are limited, and surface charging may occur. The latter is also true, when the growing film is insulating. By using pulsed bias, one allows the plasma to deliver charge-compensating electrons during bias-off

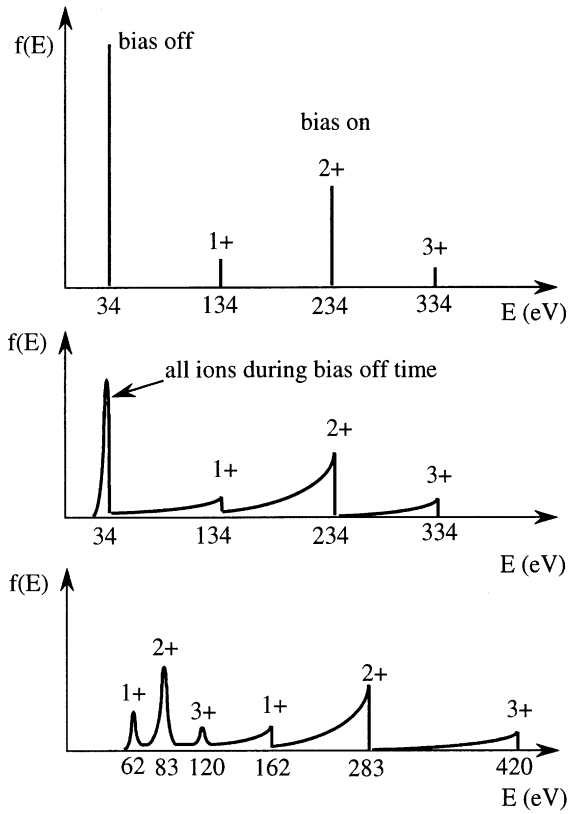

Fig. 2. Energy distribution for the MePIIID process assuming, as an example, gold plasma and –100 V bias: Top: idealized distribution of the kinetic ion energy for bias off-(left peak) and on-time (three right peaks); Center: time-averaged distribution of the kinetic energy with significant pulse rise and fall times; Bottom: as center, but total energy, i.e. taking ionization energies and cohesive energy into account.

periods. Some researchers proposed the use of bipolar bias to assist charge compensation. Energetic deposition is therefore not limited to conducting substrates [33].

3. Effects of energetic film growth conditions on film properties

The effects of film growth conditions on film properties have been often reviewed [9,34–39] and therefore, we focus here on energetic deposition using filtered arc plasmas and the MePIIID technique.

3.1. Creation of an intermixed layer; adhesion

Film growth starts with substrate preparation and nucleation. In MePIIID, the very same setup can be used for the initial stages. A higher bias voltage and a greater bias duty cycle are beneficial as compared to the later film growth stage. The idea is to optimize the ion energy for maximum sputter rate thereby removing surface layers such as water, oxides, etc. and creating dangling bonds. Sputter yields are maximum for ion energies of order 1–5 keV, the specifics depend on the ion-substrate pair and other details. Sputter yields can be found in textbooks [40] and calculated, for instance, by Monte Carlo codes such as TRIM [3,41].

The beneficial effects of an intermixed layer on improved adhesion were already pointed out in the early works of MePIIID by Brown [28]. The effect of an intermixed layer between a vacuum-arc-deposited carbon film and a silicon substrate was investigated [42]. Tarrant and coworkers applied the Griffith criterion [43] for crack propagation in bulk materials to the film delamination problem and reformulated that a film has the potential to delaminate if the strain energy released by delamination per unit area exceeds the adhesion energy per unit area [44,45]. The adhesion energy is equivalent to the energy needed to form the two new surfaces by delamination. By creating an intermixed layer with energetic ions, the adhesion energy is increased. This statement can be supported by several arguments. First, the number of bonds per unit area between the two materials is increased for geometrical reasons: an intermixed layer is similar to an atomically rough interface. In the picture of surface energy, the number of dangling bonds per area is larger for a rough surface than for atomically flat surface. The argument is still true when considering that the dangling bonds may be relaxed. Second, when the intermixed layer is formed, weakly bonded contaminations (water, hydrocarbons, etc.) are removed by sputtering. These contaminations would have terminated dangling bonds upon delamination and created a surface of lower energy. Absence of contamination therefore prevents the lowering of the surface energy (adhesion

energy). The two arguments refer to the adhesion energy but energetic deposition also affects the strain energy, i.e., the other part of the Griffith criterion. Here, the situation is complicated because there exists a maximum of stress as a function of ion energy (see point 3.3).

The greater the ion energy, as determined by Eq. (1), the greater is the projected range and the thicker is the intermixed layer. Based on the preceding arguments, one can expect that there is an initial strong increase in adhesion with increasing energy of film-forming ions. A further increase of ion energy will not enhance the adhesion energy but will reduce strain energy (see point 3.3).

Finally, because there is no sharp interface between the materials, the strain at the interface is distributed over a larger number of atoms per unit area. A gradual transition from one material to another can better accommodate the strain associated with lattice mismatch or film stress. These rather qualitative arguments are the subject of research and it can be anticipated that molecular dynamics and other techniques will clarify the details of adhesion and delamination.

3.2. Nucleation

Interface formation is closely related to nucleation of the growing film. Important factors include (i) the surface temperature, affecting the mobility of surface atoms, (ii) the kinetic ion energy, determining the projected range or penetration depth, sputtering, and motion of atoms on the surface, and (iii) the surface composition, affecting the details of sputtering. The nucleation stage is of particular importance to ultrathin (a few nm) films, because film growth is practically stopped when the nucleation stage is completed. Examples of ultrathin films include amorphous carbon films on magnetic multilayers and transparent conducting layers. There are only a few studies on nucleation using cathodic arc plasmas and the MePIIID technique.

Chun and Chayahara [46] investigated nucleation of gold on glassy carbon, mica, and glass at room temperature, using pulsed vacuum arcs and pulse bias. Without the bias applied, they found nucleation to be similar to the conventional Vollmer–Weber mode, starting with island growth and forming a continuous film when the thickness reached 80 nm. With pulsed bias up to -5 kV, resputtering balances deposition after a thin intermixed layer was formed. Therefore, regardless of the arc pulse number, the film remained at a nominal thickness of 3 nm as determined by Rutherford Backscattering Spectroscopy. Unfortunately, no details were given regarding bias pulse length and duty cycle used. By dynamic TRIM simulations, it was shown that net film growth critically depends on the bias duty cycle [30].

Durand and coworkers [5] used mass-selected ion-beam deposition to study the nucleation of energetic (100 eV) carbon ions on pyrolytic graphite from room temperature to 300°C. Islands are smaller and more numerous at room temperature due to the temperature dependence of surface diffusion. Islands are seen as roughened areas with 1–2 monolayers height. The term "island" is used even for energetic ions that penetrated the surface rather than those attached to it. There is no proof that the islands are made from the material energetically condensed. One may speculate that the islands seen in the scanning tunneling microscope are formed by atoms pushed up by the ions that penetrated the surface.

3.3. Growth mode, density, morphology, texture and stress

With ion energies in the 10 s of eV (without bias) and higher (with bias), the growth mode can be tuned by the specific choice of bias amplitude, bias pulse duration, and duty cycle. This opens a wide parameter field that is certainly not yet fully explored.

Very detailed investigations have been done for the growth of tetrahedral amorphous carbon (ta-C) films both experimentally [47–50] and theoretically [51–54]. Lossy and coworkers [47,48] showed already in the early 1990s that the sp^3 content of vacuum arc-deposited ta-C can be $>80\%$, hence, the term "amorphous diamond." Today, it is widely accepted that an optimum energy of about 100 eV leads to a maxima in properties such as sp^3 fraction, density, stress, optical band gap, and resistivity. The subplantation (very

shallow implantation) model [51,52] describes film growth from under the surface rather than on the surface. Interestingly, the basic concept of subplantation can be extended to materials other than carbon [7], i.e., practically all materials show effects like densification and stress development.

It is well known that films deposited by low-energy species (evaporation) have voids, a columnar structure, and exhibit tensile stress [36]. Increasing the energy of the film-forming species beyond thermal energies, or supplying assisting energetic ions, promotes surface mobility of atoms, forward sputtering, and film densification, leading to a reduction of tensile stress and then sharply in compressive stress (Fig. 3) [36]. The compressive stress is maximum at roughly 50–100 eV per arriving ion and is reduced at higher energies [55]. The energy values are for orientation only; they depend, of course, on the specific material. Investigating arc-deposited TiN films on silicon for instance, Bendavid and coworkers [56] found a reduction of compressive stress with a substrate bias as low as –50 V for a deposition temperature of 375°C and a rate of 6 μm/h. For arc-deposited Cr–N, a reduction in compressive stress was found for bias higher than –100 V [57], and for (Ti,Al)N films the reduction was observed for bias greater than –200 V [22]. As pointed out by Zhitomisky for arc-deposited TiN [58] and ZrN [59], one has to be careful when interpreting film data as a function of substrate bias, because not only the ion energies are increased, but also the film growth temperature. For instance, the stress curve mentioned for Cr–N coatings [57] includes films grown at temperatures from 200°C to 420°C.

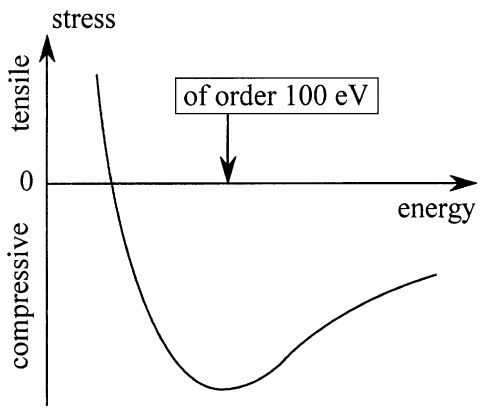

Fig. 3. Schematic presentation of film stress as a function of the average energy of film-forming particles.

The differences in the stress curves are primarily due to the specifics of the material system, and are also influenced by the deposition rate and temperature. However, strictly speaking, there is no single temperature value in the case of energetic deposition. Temperature can only be understood in a local, time-dependent sense because the impact of each energetic ion creates a small volume of enhanced temperature. For the very high energies of ion implantation, the small volume is determined by the collision cascades and is known to quench in just some picoseconds (thermal spike model). At much lower energies typical for MePIIID and other energetic deposition techniques, the thermal spike volumes involve only a relatively small number of atoms, and the process can be described as atomic scale heating (ASH). Musil [13] pointed out that ASH can replace conventional heating and thus produce dense films corresponding to zone "T" in the Thornton structural zone model [1] when sputtering is carried out at a low pressure of about 0.1 Pa and even lower. Kelires [54] proposed to use a local atomic level stress tensor when calculating structures of hard, amorphous materials. ASH should greatly influence the local atomic level stress tensor.

For energetic deposition using fully ionized plasmas and the MePIIID technique, we need to take into account that the arriving ions not only have considerable kinetic energy, but also potential energy. Since other film deposition techniques do not use fully ionized plasmas, the contribution of the potential energy is usually not important and not considered. The potential energy includes ionization energies, excitation energy, and the cohesive energy. The total energy of an ion of charge state Q arriving at the substrate surface is given by

$$E(Q,t) = E_{kin,0} + QV_{bias}(t) + \sum_{Q'=0}^{Q-1} E_{Q'} + E_{exc} + E_c, \quad (2)$$

where the first two terms are the kinetic energy as mentioned in Eq. (1), E_{exc} is the excitation energy of bound electrons in excited states, or rotation and vibration energies if the arriving ion is a molecule, and is E_c the cohesive energy. Generally, the excitation energy is negligible and mentioned here for completeness only. The ionization energies are significant, especially for multiply charged ions. Note that the ionization energy E_Q is defined as the energy needed to remove a bound electron from an ion of charge state Q, forming an ion of charge state to $Q+1$ [60,61]. Therefore, when calculating the total ionization energy being supplied to the substrate by, say, a triply charged ion, one needs to add the ionization energies of all three ionization steps, as shown in Eq. (2). Table 1 includes ionization energies and cohesive energies. For deposition from filtered cathodic arc plasmas, the difference between kinetic and total energy, Eqs. (1) and (2), respectively, can be quite important; compare Fig. 2 center and bottom.

The greater the ionization state, the higher is the potential energy, and the potential energy may exceed the kinetic energy for highly charged ions. For instance, the potential energy of highly charged ions produced by an electron beam ion trap (EBIT) can cause electron emission and significant electronic excitation of the substrate material [62].

While the transition from tensile to compressive stress has been extensively studied for sputtering and ion-assisted deposition [36,37,55,63], the nature of stress relaxation at a higher energy is less investigated and utilized. Possible reasons for the lack of attention are perhaps the reduced deposition rate due to sputtering as well as unwanted ion damage and amorphization that are observed at higher energies. The self-sputter yield reaches unity for ion energies of order 1 keV, thus a film growth at higher energies occurs only at a low percentage of energetic ions.

In a recent work, Bilek and coworkers [45] associated stress relaxation at much higher ion energies (keV) with the thermal spike model. The higher the impact energy, the greater is the volume of the thermal spike and the longer is the quenching time. For sufficiently high-ion energy, atoms are given the energy and time to move to different configurations and thus relax stress by assuming positions of minimum free energy. For carbon, this would promote relaxation from sp^3 to sp^2 hybridization, in agreement with observations [64].

MePIIID and other techniques offer the possibility to choose bias amplitude and duty cycle so as to adjust the ion energy and the ratio of high-energy to low-energy particles. Very high-ion energy at very low duty cycle produces stress relaxation [45,55,64]. Stress relaxation by energetic self-ion bombardment can be used to grow thick films that would otherwise delaminate. The most prominent example is the growth of thick layers of hard amorphous carbon. Stress relaxation can be achieved by thermal annealing with a carefully chosen temperature and a procedure that maintains the diamond-like character of the films [65,66]. However, the energy of ions can also be used, provided it is sufficiently high to cause tress relaxation by defect recombination and reduction of strain energy. In earlier works of cathodic arc deposition [42,67], good adhesion was associated with the formation of an intermixed layer (see 3.1.), however, stress relaxation most likely contributed to the observations (Fig. 4). Vacuum arc deposition of μm-thick hard carbon films was made possible using very high carbon ion energy (20 keV) at a very low duty cycle (1%) [68].

By affecting film density and stress, energetic deposition also has a profound influence on practically all properties, including hardness, Young's modulus, surface roughness, and texture. Depending on the material and temperature, films are either amorphous or polycrystalline. A thermodynamic description can be used to determine the preferred texture and orientation, taking into account surface energies, energy at interfaces, and elastic strain energy [69]. If the deposition is performed at a relatively low temperature, where atoms are not able to move to many configurations at times much longer than the thermal spike quenching time, the structures are determined by the effects of the impacting ions, particularly by the impact-induced strain energy. This non-equilibrium, kinetic growth mode is especially important for the deposition of some superhard materials such as ta-C [50,70] and c-BN [71–73].

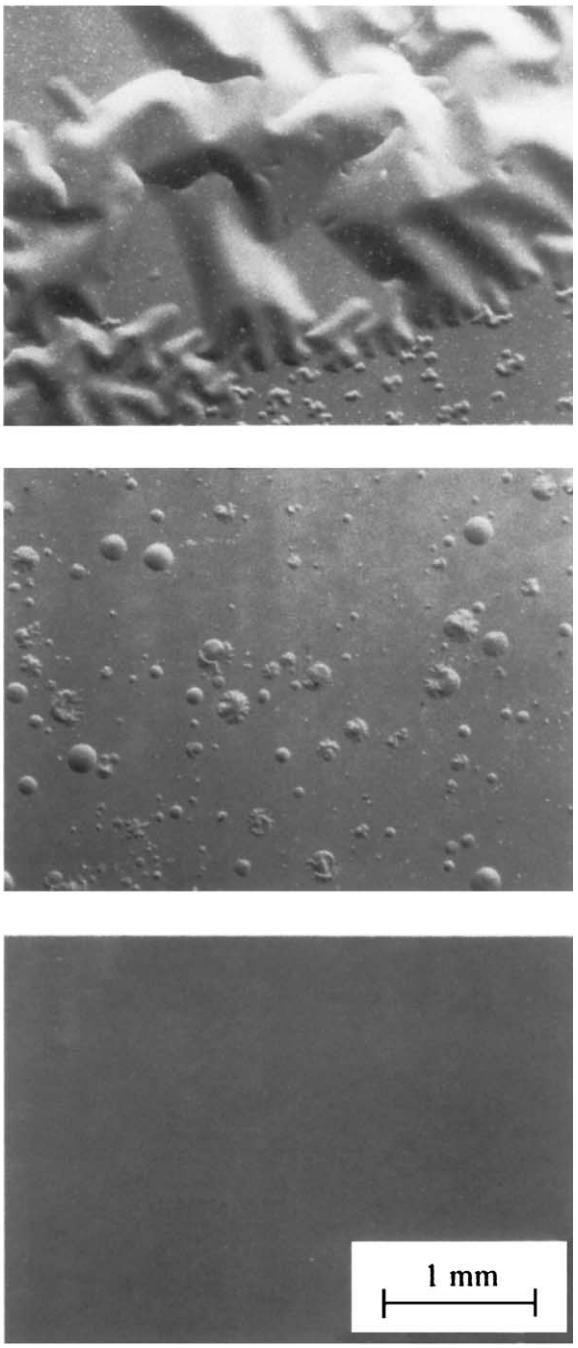

Fig. 4. Effect of ion energy on delamination: A 100 nm thick film of $YBa_2Cu_3O_x$ was deposited by filtered cathodic arc on a silver layer that was previously deposited on a silicon wafer. Top: no bias is applied; Center, pulsed bias –200 V, 2 μs; Bottom: pulsed bias –2 kV, 2 μs (from [67]).

4. Some applications

4.1. Ultrathin carbon films for data storage applications

For many years, the magnetic storage industry has demonstrated a remarkable increase in data storage density; research and development is currently undergoing towards 100 Gbit/in^2, allowing consumers to buy hard disk drives that will have several 100 Gbytes [74]. In order to achieve this, the read/write head has to be extremely close ($\sim$10 nm) to the magnetic layers of the disks; thus, protective coatings such as ultrathin ta-C layers have to be as thin as 3 nm or less. Energetic deposition of carbon ions produced by a filtered cathodic arc has been shown to be a promising approach to reach these goals [75,76].

4.2. Thick carbon films for MEMS applications

As mentioned in point 3.3, stress relaxation can be used to grow thick hard carbon films that still have their diamond-like character [65,66,68]. Possible applications are microelectromechanical systems (MEMS) where materials are needed that are tough, i.e. hard and elastic, chemically inert, showing low friction and wear, and are compatible with other application-specific requirements.

4.3. Dense metal films as laser mirrors

The columnar film structure obtained by evaporation or sputtering implies less than perfect reflection of radiation. The reflectivity can be improved by ion assistance such as energetic self-ion assistance of cathodic arc deposition. For instance, Martin and coworkers [77] increased the reflectivity of gold films in the near-IR region from 96% by magnetron sputtering to 99% using filtered cathodic arc gold plasma. Although this increase does not seem to be much, it can be critical for high-power laser applications.

4.4. Improvement of environmental stability of optical films

The properties of optical films such as the index of refraction and the coefficient of absorption depend on the film density and texture. Energetic deposition determines even optical film properties of oxides and nitrides [77]. Porosity found in films fabricated by evaporation facilitates film degradation, particularly in humid environments, and thus energetically deposited films exhibit a better long-term performance. For instance, the porosity of silver films was shown to be reduced by ion-assisted deposition, leading to improved stability in humid environments [78].

4.5. Transparent conducting films

There are at least two types of transparent conducting films: thin metal films and conducting oxide films such as indium tin oxide (ITO) and ZnO. These films are of great importance for low-emissivity glass windows, touch-screens, solar cells, and electrochromic devices. The oxide films usually show a very high transmission in the visible region, but reflect in the infrared. Energetic deposition has an effect on both optical and electrical performance.

Thin conducting metal films should be made from noble metals to prevent rapid degradation by oxidation. Ultrathin platinum films show increased conductivity when deposited with substrate bias of at least –100 V. For instance, a resistivity of $66\,\mu\Omega\,cm^{-1}$ was obtained for film thickness of 5 nm having 40% transmission at the He–Ne wavelength of 632.8 nm [79,80].

ZnO is a wide band gap semiconductor that shows good conducting properties when doped, for instance, with Al. Xu and coworkers [81] used filtered cathodic arc deposition to fabricate high-quality polycrystalline ZnO on Si (1 0 0) substrates.

4.6. Metallization of semiconductors

Energetic deposition is rarely used in the semiconductor industry, mainly because ion energy causes ion damage (defects) of the growing crystalline films. For some fabrication processes, however, these defects can be "repaired" by annealing, as it is commonly done after ion implantation. It has been demonstrated [82] that energetic deposition using filtered vacuum arc plasmas can lead to copper filling of vials and trenches as well as to the conformal deposition of diffusion barrier layers. Using the MePIIID technique with optimized parameters, Monteiro [83] conformally deposited Ta and TaN barrier layers and filled 100 nm wide trenches of 8:1 aspect ratio with copper. Energetic deposition other than filtered arc and MePIIID, however, is used in the semiconductor industry. In "ionized physical vapor deposition" (I-PVD), metal vapor from an evaporation source or sputter target is ionized using ECR or RF discharges. The ions are accelerated by a bias up to –150 V and can be used to fill vials and trenches [11].

4.7. Deposition of hard and protective coatings

Tools, engine components, building appliances, biomedical implants, and many other workpieces are being coated with cathodic arc and other energetic deposition technologies [1,2,8,26,84]. The purpose is to form highly adherent coatings that protect the bulk material against wear and corrosion. From this very large field, only a few examples shall be mentioned. Some oxide and nitride films show high-corrosion resistance, hardness, elasticity and a low coefficient of friction [56,77]. TiN and (Ti,Al)N coatings are today commercially deposited using Ti and Ti–Al DC-cathodic arcs in a nitrogen environment and with substrate biasing. Al_2O_3 films were deposited on stainless steel using a filtered arc [85] and pulsed high-voltage substrate bias [28]. A dual-plasma-source approach was demonstrated for the energetic deposition mullite, a coating that protects against oxidation at a high temperature [86]. Other coatings are being developed such as c-BN [71] and nanocomposite coatings [13]. Recently, there are also efforts to deposit B_4C films using cathodic arcs [87].

5. Summary and conclusion

Energetic deposition in the form of ion plating and ion-assisted deposition has been recognized for many years as powerful methods for the fabrication of dense films with tailored mechanical, tribological, optical, chemical, etc., properties. In recent years, energetic self-ion-assisted deposition such as the MePIIID technique and hybrid implantation and deposition methods have emerged. Particularly interesting is the relation of ion energy and stress, which in turn affects strain energy, adhesion, texture, hardness, elastic modulus, index of refraction, and other film properties. For MePIIID and similar techniques using fully ionized plasmas, one needs to distinguish between the kinetic ion energy on the one hand, which is important for the formation of an intermixed layer, sputtering, and the subplantation growth mechanism, and the total ion energy on the other hand, determining substrate heating via atomic scale heating, and associated effects such as stress relaxation.

Acknowledgements

The author gratefully acknowledges stimulating discussions with Othon Monteiro, Berkeley, Marcela Bilek, Sydney, and Marie-Paule Delplancke-Ogletree, Brussels. This work was supported by the US Department of Energy, under Contract No. DE-AC03-76SF00098.

References

[1] Bunshah RF, editor. Handbook of deposition technologies for films and coatings: science, technology, and applications. 2nd ed. Park Ridge, NJ: Noyes, 1994.
[2] Schneider JM, Rohde S, Sproul WD, Matthews A. J Phys D 2000;33:R173–86.
[3] Eckstein W. Computer simulation of ion–solid interactions. Berlin: Springer, 1991.
[4] Küttel OM, Groening P, Agostino RG, Schlapbach L. J Vac Sci Technol A 1995;13:2848–55.
[5] Durand HA, Sekine K, Etoh K, Ito K, Kataoka I. J Appl Phys 1998;84:2591–6.
[6] Ohno H, van der Berg JA, Nagai S, Armour DG. Nucl Instrum and Methods B 1999;148:673–7.
[7] Enders B, Heck C, Tsubouchi N, Chayahara A, Kinomura A, Horino Y, Fujii K. Nucl Instrum Methods B 1999; 148:143–8.
[8] Rossnagel SM, Cuomo JJ, Westwood WD, editors. Handbook of plasma processing technology. Westwood, NJ: Noyes, 1990.
[9] Cuomo JJ, Rossnagel SM, Kaufman HR, editors. Handbook of ion beam processing technology. Park Ridge, NJ: Noyes, 1989.
[10] Rossnagel SR, Hopwood J. J Vac Sci Technol B 1994; 12:449–53.
[11] Rossnagel SM. J Vac Sci Technol B 1998;16:2585–608.
[12] Bratzsch H, Frach P, Goedicke K, Gottfried C. Surf Coat Technol 1999;120–121:723–7.
[13] Musil J. Surf Coat Technol 2000;125:322–30.
[14] Miller JC, editor. Laser ablation: principles and applications. Berlin and New York: Springer, 1994.
[15] Jordan R, Cole D, Lunny JG, Mackay K, Givord D. Appl Surf Sci 1995;86:24–8.
[16] Chrisey DB, Hubler GK, editors. Pulsed laser deposition of thin films. New York: Wiley, 1994.
[17] Jüttner B, Puchkarev VF, Hantzsche E, Beilis I. Cathode spots. In: Boxman RL, Sanders DM, Martin PJ, editors. Handbook of vacuum arc science and technology. Park Ridge, NJ: Noyes, 1995. p. 73–281.
[18] Anders A, Yotsombat B, Binder R. J Appl Phys 2001; 89:7764–71.
[19] Edison TA, Art of plating one material with another. Patent US 526,147, September 18, 1894 (filed January 28, 1884).
[20] Aksenov II, Belous VA, Padalka VG. Instrum Exp Tech 1978;21:1416–8.
[21] Anders A. Surf Coat Technol 1999;120–121:319–30.
[22] Cheng YH, Tay BK, Lau SP, Shi X. J Vac Sci Technol A 2001;19:736–42.
[23] Mattox DM. Ion plating. In: Bunshah RF, editor. Handbook of deposition technologies for films and coatings. Westwood NJ: Noyes, 1994. p. 320–73.
[24] Adler RJ, Picraux ST. Nucl Instrum Methods B 1985;6:123–8.
[25] Conrad JR, Radtke JL, Dodd RA, Worzala FJ, Tran NC. J Appl Phys 1987;62:4591–6.
[26] Anders A, editor. Handbook of plasma immersion ion implantation and deposition. New York: Wiley, 2000.
[27] Brown IG, Godechot X, Yu KM. Appl Phys Lett 1991; 58:1392–4.
[28] Brown IG, Anders A, Anders S, Dickinson MR, Ivanov IC, MacGill RA, Yao XY, Yu K-M. Nucl Instrum Methods B 1993;80/81:1281–7.
[29] Anders A. Surf Coat Technol 1997;93:157–67.
[30] Anders A, Anders S, Brown IG, Yu KM. In-situ deposition of sacrificial layers during ion implantation: concept and simulation. In: Williams JS, Elliman RG, Ridgway MC, editors. Ion beam modification of materials. Amsterdam: Elsevier, 1996. p. 1089–92.
[31] Yushkov GY, Anders A, Oks EM, Brown IG. J Appl Phys 2000;88:5618–22.

[32] Anders A. IEEE Trans Plasma Sci 2001;29:393–8.
[33] Iskanderova ZA, Kleinman JI, Gudimenko Y, Tkachenko A, Tennyson RC, Brown IG, Monteiro OR. Nucl Instrum Methods 1999;148:1090–6.
[34] Auciello O, Kelly R, editors. Ion bombardment modification of surfaces. Amsterdam: Elsevier, 1984.
[35] Mattox DM. J Vac Sci Technol A 1989;7:1105–14.
[36] Thornton JA, Hoffman DW. Thin Solid Films 1989;171: 5–31.
[37] Windischmann H. J Vac Sci Technol A 1991;9:2431–6.
[38] Colligon JS. J Vac Sci Technol A 1995;13:1649–57.
[39] Monteiro OR. Annu Rev Mater Sci 2001;31:111–37.
[40] Behrisch R, editor. Sputtering by particle bombardment I. Berlin: Springer, 1981.
[41] Ziegler JF, Biersack JP, Littmark U. The stopping and range of ions in solids. New York: Pergamon Press, 1985.
[42] Gerstner EG, McKenzie DR, Puchert MK, Timbrell PY, Zou J. J Vac Sci Technol A 1995;13:406–11.
[43] Griffith AA. Phil Trans Roy Soc A 1920;221:163–98.
[44] Tarrant RN, Montross CS, McKenzie DR. Surf Coat Technol 2001;136:188–91.
[45] Bilek MMM, McKenzie DR, Tarrant RN, Lim SHN, McCulloch DG. Surf Coat Technol 2002, submitted for publication.
[46] Chun S, Chayahara A. Surf Coat Technol 2001;137: 241–5.
[47] Lossy R, Pappas DL, Roy RA, Doyle JP, Bruley J. J Appl Phys 1995;77:4750–6.
[48] Lossy R, Pappas DL, Roy RA, Cuomo JJ, Sura VH. Appl Phys Lett 1992;61:171–3.
[49] Pharr GM, Callahan DL, McAdams D, Tsui TY, Anders S, Anders JW, Ager I, Brown G, Bhatia CS, Silva SRP, Robertson J. Appl Phys Lett 1996;68:779–81.
[50] Chhowalla M, Robertson J, Chen CW, Silva SRP, Davis CA, Amaratunga GAJ, Milne WI. J Appl Phys 1997; 81:139–45.
[51] Lifshitz Y, Kasai SR, Rabalais JW, Eckstein W. Phys Rev B 1990;41:10468–80.
[52] McKenzie DR, Muller D, Pailthorpe BA. Phys Rev Lett 1991;67:773–6.
[53] Jäger HU, Albe K. J Appl Phys 2000;88:1129–35.
[54] Kelires PC. Phys Rev B 2000;62:15686–94.
[55] Nastasi M, Möller W, Ensinger W. Ion implantation and thin-film deposition. In: Anders A, editor. Handbook of plasma immersion ion implantation and deposition. New York: Wiley, 2000. p. 125–241.
[56] Bendavid A, Martin PJ, Netterfield RP, Kinder TJ. Surf Coat Technol 1994;70:97–106.
[57] Odén M, Almer J, Håkansson G. Surf Coat Technol 1999;120–121:272–6.
[58] Zhitomirsky VN, Grimberg I, Rapoport L, Boxman RL, Travitzky NA, Goldsmith S, Weiss BZ. Surf Coat Technol 2000;133–134:114–20.
[59] Zhitomirsky VN, Grimberg I, Boxman RL, Travitzky NA, Goldsmith S, Weiss BZ. Surf Coat Technol 1997;94–95:207–12.
[60] Carlson TA, Nestor CW, Wasserman N, McDowell JD. Atomic Data 1970;2:63–99.
[61] Lide DR, editor. Handbook of chemistry and physics. 81st ed. Boca Raton, New York: CRC Press, 2000.
[62] Schenkel T, Barnes AV, Niedermayr TR, Hattass M, Newman MW, Machicoane GA, McDonald JW, Hamza AV, Schneider DH. Phys Rev Lett 1999;83:4273–6.
[63] Hudson C, Somekh RE. J Vac Sci Technol A 1996; 14:2169–74.
[64] Khan RUA, Silva SRP. Diamond Relat Mater 2001; 10:224–9.
[65] Friedmann TA, Sullivan JP, Knapp JA, Tallant DR, Follstaedt DM, Medlin DL, Mirkarimi PB. Appl Phys Lett 1997;71:3820–2.
[66] Monteiro OR, Ager III JW, Lee DH, Lo RY, Walter KC, Nastasi M. J Appl Phys 2000;88:2395–9.
[67] Anders A, Anders S, Brown IG, Dickinson MR, MacGill RA. J Vac Sci Technol B 1994;12:815–20.
[68] Tarrant RN, Fujisawa N, Swain MV, James NL, McKenzie DR, Woodward JC. Surf Coat Technol 2002, submitted for publication.
[69] McKenzie DR, Bilek MMM. Thin Solid Films 2001;382:280–7.
[70] McKenzie DR, Muller D, Pailthorpe BA, Wang ZH, Kravtchinskaya E, Segal D, Lukins PB, Swift PD, Martin PJ, Amaratunga G, Gaskell PH, Saeed A. Diamond Relat Mater 1991;1:51–9.
[71] Hofsäss H, Feldermann H, Sebastian M, Ronning C. Phys Rev B 1997;55:13230–3.
[72] Reinke S, Freudenstein R, Kulisch W. Surf Coat Technol 1997;97:263–9.
[73] Klett A, Freudenstein R, Plass MF, Kulisch W. Surf Coat Technol 1999;116–119:86–92.
[74] Goglia PR, Berkowitz J, Hoehn J, Xidis A, Stover L. Diamond Relat Mater 2001;10:271–7.
[75] Anders S, Brown IG, Bhatia CS, Bogy DB. Data Storage 1997;4:31–8.
[76] Anders A, Fong W, Kulkarni A, Ryan FR, Bhatia CS. IEEE Trans Plasma Sci 2001;29:768–75.
[77] Martin PJ, Bendavid A, Netterfield RP, Kinder TJ, Jahan F, Smith G. Surf Coat Technol 1999;112: 257–60.
[78] Lee C, Lee T, Jen Y. Thin Solid Films 2000;359:95–7.
[79] Avrekh M, Thibadeau BM, Monteiro OR, Brown IG. Rev Sci Instrum 1999;70:4328–30.
[80] Avrekh M, Monteiro OR, Brown IG. Appl Surf Sci 2000;158:217–22.
[81] Xu XL, Lau SP, Chen JS, Chen GY, Tay BK. J Cryst Growth 2001;223:201–5.
[82] Siemroth P, Wenzel C, Kliomes W, Schultrich B, Schülke T. Thin Solid Films 1997;308:455–9.
[83] Monteiro OR. J Vac Sci Technol B 1999;17:1094–7.
[84] Boxman RL, Sanders DM, Martin PJ. Handbook of vacuum arc science and technology. Park Ridge NJ: Noyes, 1995.
[85] Randhawa H. J Vac Sci Technol A 1989;7:2346–9.

[86] Monteiro OR, Wang Z, Brown IG. J Mater Res 1997; 12:2401–10.
[87] Klepper CC, Niemel J, Hazelton RC, Yadlowsky EJ, Monteiro OR. Fusion Technol 2001;39:910–5.
[88] Kittel C. Introduction to solid state physics. New York: Wiley, 1986.
[89] Anders A, Yushkov GY. J Appl Phys 2002;91: 4824–32.
[90] Brown IG. Rev Sci Instrum 1994;65:3061–81.
[91] Oks EM, Anders A, Brown IG, Dickinson MR, MacGill RA. IEEE Trans Plasma Sci 1996;24:1174–83.